Inorg. Chem. **2006**, *45*, 9721–9728

Low-Spin Bis(2-methylimidazole)(octaethylporphyrinato)iron(III) Chloride (*perp*-[Fe(OEP)(2-MeHIm)$_2$]Cl): A Consequence of Hydrogen Bonding?

Chuanjiang Hu,[†] Bruce C. Noll,[†] Charles E. Schulz,[‡] and W. Robert Scheidt*,[†]

Department of Chemistry and Biochemistry, University of Notre Dame, Notre Dame, Indiana 46556, and Department of Physics, Knox College, Galesburg, Illinois 61401

Received June 7, 2006

The synthesis and characterization of low-spin bis(2-methylimidazole)(octaethylporphyrinato)iron(III) chloride (*perp*-[Fe(OEP)(2-MeHIm)$_2$]Cl) is reported. The structure shows that the cation is a low-spin species with two imidazole ligands having a relative perpendicular orientation. The porphyrin core is very ruffled, which leads to shortened equatorial bonds of 1.974(4) Å and slightly elongated axial Fe–N bond lengths of 2.005(10) Å that are about 0.02 Å shorter and 0.03 Å longer, respectively, in comparison to bis-imidazole ligated iron(III) species with parallel oriented axial ligands. A one-dimensional hydrogen-bond chain is formed between chloride anions and uncoordinated imidazole nitrogen atoms. Compared with *paral*-[Fe(OEP)(2-MeHIm)$_2$]ClO$_4$, hydrogen bonding may play an important role in the differences in the two structures. Mössbauer spectra show broadened quadrupole doublets with quadrupole splittings of 1.81 mm/s at RT and 1.94 mm/s at 20 K. The isomer shift ranges from 0.26 to 0.36 mm/s. These confirm that the title complex is a low-spin iron(III) species with the ground state $(d_{xy})^2(d_{xz},d_{yz})^3$. Crystal data: monoclinic, space group $P2_1/c$, $a = 14.066(3)$ Å, b, 20.883(4) Å, $c = 19.245(4)$ Å, $\beta = 109.67°$, and $Z = 4$.

Introduction

Bis-histidine-coordinated hemes have been of interest due to their importance in electron-transfer biological systems. In current protein structures, two limiting orientations of the axial ligand planes are found: imidazole planes oriented parallel to each other (cytochromes b_5,[1] three of the heme centers of cytochromes c_3,[2−4] the *b* hemes of sulfite oxidase[5] and flavocytochrome b_2,[6] and the heme *a* of cytochrome oxidase[7]) while one of the four heme groups in cytochrome c_3 from *Desulfovibrio vulgaris* has a more staggered conformation in which the dihedral angle between the histidine planes is closer to a relative perpendicular arrangement (64°). The relative orientation of the two imidazole planes with respect to each other has been believed to play an important role in modeling the spectroscopic properties (such as EPR) and possibly also the redox properties of these heme proteins.

The orientations of planar axial ligands in bis-ligated hemes of iron(III) have been intensively investigated. The earliest studies showed that the relative and absolute orientations of the two axial ligands have significant effects on the electronic structure. The first example was that of [Fe(OEP)(3-ClPy)$_2$]ClO$_4$,[8] where two different crystalline polymorphs were isolated. The polymorphs are those of a triclinic, spin-

* To whom correspondence should be addressed. E-mail: scheidt.1@nd.edu.
[†] University of Notre Dame.
[‡] Knox College.

(1) Mathews, F. S.; Czerwinski, E. W.; Argos, P. In *The Porphyrins*; Dolphin, D., Ed.; Academic Press: New York, 1979; Vol. VII, p 108.
(2) Pierrot, M.; Haser, R.; Frey, M.; Payan, F.; Astier, J.-P. *J. Biol. Chem.* **1982**, *257*, 14341.
(3) Higuchi, Y.; Kusunoki, M.; Matsuura, Y.; Yasuoka, N.; Kakudo, M. *J. Mol. Biol.* **1984**, *172*, 109.
(4) Czjzek, M.; Guerlesquin, F.; Bruschi, M.; Haser, R. *Structure* **1996**, *4*, 395.
(5) Kipke, C. A.; Cusanovich, M. A.; Tollin, G.; Sunde, R. A.; Enemark, J. H. *Biochemistry* **1988**, *27*, 2918.
(6) (a) Xia, Z.-X.; Shamala, N.; Bethge, P. H.; Lim, L. W.; Bellamy, H. D.; Xuong, N. H.; Lederer, F.; Mathews, F. S. *Proc. Natl. Acad. Sci. U.S.A.* **1987**, *84*, 2629. (b) Dubois, J.; Chapman, S. K.; Mathews, F. S.; Reid, G. A.; Lederer, F. *Biochemistry* **1990**, *29*, 6393.
(7) Iwata, S.; Ostermeier, C.; Ludwig, B.; Michel, H. *Nature (London)* **1995**, *376*, 660.

(8) The following abbreviations are used in this paper: TMP, dianion of *meso*-tetramesitylporphyrin; TPP, dianion of *meso*-tetraphenylporphyrin; Proto IX, dianion of protoporphyrin IX.; t-Mu, *trans*-methylurocanate; c-Mu, *cis*-methylurocanate; OMTPP, dianion of octamethyltetraphenylporphyrin; OETPP, dianion of octaethyltetraphenylporphyrin; RIm, a generalized hindered imidazole; HIm, imidazole; 1-MeIm, 1-methylimidazole; 2-MeHIm, 2-methylimidazole; 4-MeHIm, 4-methylimidazole; 5-MeHIm, 5-methylimidazole; 1,2-Me$_2$Im, 1,2-dimethylimidazole; Py, pyridine; 3-ClPy, 3-chloropyridine; 4-CNPy, 4-cyanopyridine; 3-CNPy, 3-cyanopyridine; 4-MePy, 4-methylpyridine; 3-EtPy, 3-ethylpyridine; 4-NMe$_2$Py, 4-(dimethylamino)pyridine; N_p, porphyrinato nitrogen; Ct, the center of four porphyrinato nitrogen atoms; N_{Ax}, nitrogen of axial ligands; N_{im}, nitrogen of imidazole ligands; C_{im}, carbon of imidazole ligands.

10.1021/ic061014u CCC: $33.50
Published on Web 10/27/2006

equilibrium ($S = 1/2 \rightleftharpoons S = 5/2$)[9,10] system and a monoclinic, intermediate-spin system, $S = 3/2$.[11] In these complexes, the two pyridines maintain a relative parallel orientation but the absolute orientation of the two axial ligands with respect to the porphinato core changed. Although this system showed large changes in the electronic structure of iron(III), controlling axial ligand orientation more likely will affect the relative energies of the three lowest d-orbitals of iron, namely the d_{xy}, d_{xz}, and d_{yz} orbitals.

In those model compounds, most bis-ligated d^5 iron(III) complexes have a characteristic rhombic EPR spectrum,[12] with three observed g values, while some iron(III) species have an unusual EPR spectrum: a single-feature low-spin EPR signal with $g \geq 3.2$. This EPR spectral type has been called large g_{max}[13] or highly anisotropic low-spin (HALS).[14] The origin of the large g_{max} EPR spectrum was first studied in the complex $[Fe(TPP)(2\text{-}MeHIm)_2]^+$.[15,16] This study showed that the spectrum resulted from mutually perpendicular axial ligands that lead to nearly degenerate iron d_π orbitals. Subsequently, a number of additional iron(III) species were shown to have the two planar ligands oriented perpendicular to each other.[17−19,22] Most of these species display a large g_{max} EPR spectrum[17,18,20,23] and an unusually small value of the Mössbauer quadrupole splitting constant.[16,17,19,21,22] A final case is found for strong π-accepting ligands, such as 3- and 4-cyanopyridine, where the interaction with axial ligands lowers the energy of iron d_π orbitals below d_{xy} so that the ground state changes to $(d_{xz},d_{yz})^4(d_{xy})^1$. This leads to a final type of EPR spectrum observed in low-spin iron(III): an axial EPR spectrum. All of the complexes with relative perpendicular ligands are found to have strongly ruffled porphyrinato cores. For these systems, this conformation allows for the possibility of a π interaction between iron and the porphyrin.

In addition to the above-mentioned $[Fe(OEP)(3\text{-}ClPy)_2]ClO_4$,[8] several other examples of iron(III) porphyrins with identical axial ligands that have different structure and/or physical properties have been studied.[18,24,25] Both $[Fe(TPP)(HIm)_2]^+$ and $[Fe(TMP)(5\text{-}MeIm)_2]^+$ have been shown to form two different low-spin crystalline species. They are structurally distinguished by the relative orientation of the two axial ligands. We have synthesized and structurally characterized a new bis-ligated complex, *perp*-$[Fe(OEP)(2\text{-}MeHIm)_2]Cl$. Interestingly, this new complex is a low-spin species with two perpendicular ligands that is distinct from the related complex *paral*-$[Fe(OEP)(2\text{-}MeHIm)_2]ClO_4$[26] with parallel axial ligands and a high-spin state. As expected from analogous iron(III) species, the porphyrin core in this new species is necessarily ruffled to accommodate the two sterically hindered ligands. The solid-state structure shows that the coordinated imidazole ligands form hydrogen bonds with the chloride anions and provides a probable explanation for the apparent stronger ligand field observed in this complex.

Experimental Section

General Information. All solvents were used as received. The free-base porphyrin octaethylporphyrin (H_2OEP)[8] was purchased from Mid-century. The metalation of the free-base porphyrin to give [Fe(OEP)Cl] was done as previously described.[27] $[Fe(OEP)]_2O$ was prepared according to a modified Fleischer preparation.[28]

Synthesis of *perp*-[Fe(OEP)(2-MeHIm)$_2$]Cl. To a solution of [Fe(OEP)Cl] (30 mg, 0.05 mmol) in 10 mL of chloroform, 2-methylimidazole (20 mg, 0.24 mmol) was added. The mixture was stirred for 4 h, then transferred into several 8 mm × 250 mm glass tubes, and layered by hexanes as nonsolvent for crystallization. After 10 days, block crystals were formed along with variable amount of microcrystalline materials. Samples for Mössbauer spectroscopy were made from single crystals enriched to 95% in ^{57}Fe. In addition, Mössbauer spectroscopy verified that the microcrystalline material was identical to the block crystals.

X-ray Structure Determination. A dark red crystal with the dimensions 0.46 × 0.20 × 0.12 mm^3 was used for the structure determination. The single-crystal experiment was carried out on a Bruker Apex system with graphite-monochromated Mo K_α radiation ($\lambda = 0.71073$ Å). The crystalline sample was placed in inert oil, mounted on a glass pin, and transferred to the cold gas stream of the diffractometer. Crystal data were collected at 100 K, Table 1.

The structure was solved by direct methods using SHELXS-97[29] and refined against F^2 using SHELXL-97;[30,31] subsequent difference Fourier syntheses led to the location of most of the remaining nonhydrogen atoms. For the structure refinement all data were used including negative intensities. The structure was refined in space group $P2_1/c$. The program SADABS[32] was applied for

(9) Scheidt, W. R.; Geiger, D. K. *J. Chem. Soc., Chem. Commun.* **1979**, 1154.
(10) Scheidt, W. R.; Geiger, D. K.; Haller, K. J. *J. Am. Chem. Soc.* **1982**, *104*, 495.
(11) Scheidt, W. R.; Geiger, D. K.; Hayes, R. G.; Lang, G. *J. Am. Chem. Soc.* **1983**, *105*, 2625.
(12) Blumberg, W. E.; Peisach, J. *Adv. Chem. Ser.* **1971**, *100*, 271.
(13) Walker, F. A.; Reis, D.; Balke, V. L. *J. Am. Chem. Soc.* **1984**, *106*, 6888.
(14) Magita, C. T.; Iwaizumi, M. *J. Am. Chem. Soc.* **1981**, *103*, 4378.
(15) Scheidt, W. R.; Kirner, J. L.; Hoard, J. L.; Reed, C. A. *J. Am. Chem. Soc.* **1987**, *109*, 1963.
(16) Walker, F. A.; Huynh, B. H.; Scheidt, W. R.; Osvath, S. R. *J. Am. Chem. Soc.* **1986**, *108*, 5288.
(17) Safo, M. K.; Gupta, G. P.; Walker, F. A.; Scheidt, W. R. *J. Am. Chem. Soc.* **1991**, *113*, 5497.
(18) Munro, O. Q.; Serth-Guzzo, J. A.; Turowska-Tyrk, I.; Mohanrao, K.; Shokhireva, T. Kh.; Walker, F. A.; Debrunner, P. G.; Scheidt, W. R. *J. Am. Chem. Soc.* **1999**, *121*, 11144.
(19) Munro, O. Q.; Marques, H. M.; Debrunner, P. G.; Mohanrao, K.; Scheidt, W. R. *J. Am. Chem. Soc.* **1995**, *117*, 935.
(20) Inniss, D.; Soltis, S. M.; Strouse, C. E. *J. Am. Chem. Soc.* **1988**, *110*, 5644.
(21) Safo, M. K.; Gupta, G. P.; Watson, C. T.; Simonis, U.; Walker, F. A.; Scheidt, W. R. *J. Am. Chem. Soc.* **1992**, *114*, 7066.
(22) Safo, M. K.; Walker, F. A.; Raitsimring, A. M.; Walters, W. P.; Dolata, D. P.; Debrunner, P. G.; Scheidt, W. R. *J. Am. Chem. Soc.* **1994**, *116*, 7760.
(23) Walker, F. A. *Chem. Rev.* **2004**, *104*, 589.
(24) Scheidt, W. R.; Osvath, S. R.; Lee, Y. J. *J. Am. Chem. Soc.* **1987**, *109*, 1958.
(25) Collins, D. M.; Countryman, R.; Hoard, J. L. *J. Am. Chem. Soc.* **1972**, *94*, 2066.
(26) Geiger, D. K.; Lee, Y. J.; Scheidt, W. R. *J. Am. Chem. Soc.* **1984**, *106*, 6339−6343.
(27) (a) Adler, A. D.; Longo, F. R.; Kampus, F.; Kim, J. *J. Inorg. Nucl. Chem.* **1970**, *32*, 2443. (b) Buchler, J. W. In *Porphyrins and Metalloporphyrins*; Smith, K. M., Ed.; Elsevier Scientific Publishing: Amsterdam, The Netherlands, 1975; Chapter 5.
(28) (a) Fleischer, E. B.; Srivastava, T. S. *J. Am. Chem. Soc.* **1969**, *91*, 2403. (b) Hoffman, A. B.; Collins, D. M.; Day, V. W.; Fleischer, E. B.; Srivastava, T. S.; Hoard, J. L. *J. Am. Chem. Soc.* **1972**, *94*, 3620.
(29) Sheldrick, G. M. *Acta Crystallogr.* **1990**, *A46*, 467.
(30) Sheldrick, G. M. *Program for the Refinement of Crystal Structures*; Universität Göttingen: Germany, 1997.

Table 1. Complete Crystallographic Details for [Fe(OEP)(2-MeHIm)$_2$]Cl·3CHCl$_3$

formula	$C_{47}H_{59}Cl_{10}FeN_8$
fw, amu	1146.37
a, Å	14.066(3)
b, Å	20.883(4)
c, Å	19.245(4)
β, deg	109.67(3)
V, Å^3	5323.1(18)
space group	$P2_1/c$
Z	4
D_c, g/cm^3	1.430
F(000)	2372
μ, mm^{-1}	0.827
crystal dimensions, mm	0.46 × 0.20 × 0.12
radiation	MoKα, $\bar{\lambda} = 0.71073$ Å
temp, K	100(2)
total data collected	86704
abs correction	semiempirical from equivalents
unique data	13213 ($R_{int} = 0.035$)
unique obsd data [$I > 2\sigma(I)$]	10576
refinement method	full-matrix least-squares on F^2
final *R* indices [$I > 2\sigma(I)$]	$R_1 = 0.0341$, $wR_2 = 0.0916$
final *R* indices (all data)	$R_1 = 0.0461$, $wR_2 = 0.0962$

the absorption correction. Complete crystallographic details, atomic coordinates, bond distances and angles, anisotropic thermal parameters, and fixed hydrogen atom coordinates are given in the Supporting Information.

The asymmetric unit was found to contain one iron(III) porphyrinate cation, one chloride ion, and three chloroform solvent molecules. The iron porphyrinate is a bis-ligated species, *perp*-[Fe(OEP)(2-MeHIm)$_2$]$^+$. The terminal carbon of one ethyl group is disordered over two positions. Both disordered parts (C(42(a) and C(42(b)) are refined with the same anisotropic displacement parameters and the same bond distance to C(41). After the final refinement, the occupancy of the major position was found to be 53%. All three chloroform solvent molecules are disordered over three positions. All non-hydrogen atoms were refined anisotropically. Hydrogen atoms were added with the standard SHELXL-97 idealization methods.

Results

The reaction of [Fe(OEP)Cl] with excess 2-methylimidazole yielded block crystals and microcrystalline material. The structure of the crystalline sample was determined by X-ray crystallography. The ORTEP diagram of the *perp*-[Fe(OEP)(2-MeHIm)$_2$]$^+$ cation is shown in Figure 1. The cation is a six-coordinate iron(III) porphyrinate with two relative perpendicular imidazole ligands. Selected bond distances and angles are listed in Table 2. Equatorial bond distances (Fe−N$_p$) average 1.974(4) Å. The axial bond lengths are 2.0123(15) Å and 1.9984(15) Å. The N$_{im}$−Fe−N$_{im}$ angle is 175.73(6)°.

The displacement of each atom of the porphyrin core from the 24-atom mean plane is shown in Figure 2. The orientations of the 2-MeHIm ligands including the value of the dihedral angle are also shown; the circle represents the

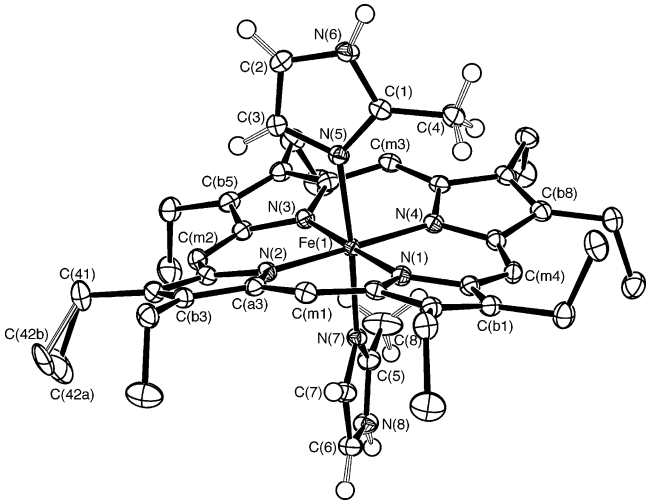

Figure 1. ORTEP diagram of six-coordinate *perp*-[Fe(OEP)(2-MeHIm)$_2$]$^+$. The hydrogen atoms of the porphyrin ligand have been omitted for clarity; the hydrogen atoms of the imidazole ligand are shown. 50% probability ellipsoids are depicted.

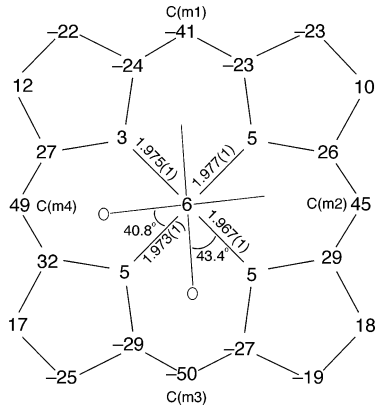

Figure 2. Formal diagram of the porphyrinato cores of *perp*-[Fe(OEP)(2-MeHIm)$_2$]$^+$. Illustrated are the displacements of each atom from the 24-atom core plane in units of 0.01 Å. The diagrams also show the orientation of the imidazole ligands with respect to the atoms of the porphyrin core. The position of the methyl group at the 2-carbon position is represented by the circle.

Table 2. Selected Bond Lengths and Angles for [Fe(OEP)(2-MeHIm)$_2$]Cl·3CHCl$_3$

bond	length (Å)	bond	length (Å)
Fe(1)−N(1)	1.9749(14)	Fe(1)−N(2)	1.9765(14)
Fe(1)−N(3)	1.9666(14)	Fe(1)−N(4)	1.9734(14)
Fe(1)−N(5)	2.0123(15)	Fe(1)−N(7)	1.9984(15)

angle	value(°)	angle	value(°)
C(a1)−N(1)−Fe(1)	127.10(11)	C(a2)−N(1)−Fe(1)	127.08(11)
C(a3)−N(2)−Fe(1)	127.03(11)	C(a4)−N(2)−Fe(1)	126.94(11)
C(a5)−N(3)−Fe(1)	127.19(11)	C(a6)−N(3)−Fe(1)	126.79(11)
C(a7)−N(4)−Fe(1)	126.49(11)	C(a8)−N(4)−Fe(1)	127.42(11)
C(1)−N(5)−Fe(1)	132.85(11)	C(3)−N(5)−Fe(1)	120.88(11)
C(5)−N(7)−Fe(1)	132.54(11)	C(7)−N(7)−Fe(1)	121.31(11)
N(7)−Fe(1)−N(5)	175.73(6)		

position of the methyl group. The six-coordinate cation has a significantly S$_4$-ruffled core. The absolute ligand orientation is given by the dihedral angle between the axial ligand plane and the closest N$_{ax}$FeN$_p$ plane and is conventionally denoted by ϕ. The ligand planes make dihedral angles of 40.8° and 43.4° to the closest N$_{ax}$FeN$_p$ plane in *perp*-[Fe(OEP)(2-MeHIm)$_2$]$^+$. The relative ligand orientation is simply the

(31) $R_1 = \sum||F_o| - |F_c||/\sum|F_o|$ and $wR_2 = \{\sum[w(F_o^2 - F_c^2)^2]/\sum[wF_o^4]\}^{1/2}$. The conventional *R* factors R_1 are based on *F*, with *F* set to zero for negative F^2. The criterion of $F^2 > 2\sigma(F^2)$ was used only for calculating R_1. *R* factors based on F^2 (wR_2) are statistically about twice as large as those based on *F*, and *R* factors based on ALL data will be even larger.

(32) Sheldrick, G. M. *Program for Empirical Absorption Correction of Area Detector Data*; Universität Göttingen: Germany, 1996.

Table 3. Selected Bond Distances (Å) and Angles (deg) for [Fe(OEP)(2-MeHIm)$_2$]Cl and Related Species[a]

complex	Fe−N$_p$[b,c]	Fe−N$_{Ax}$[c]	C$_m$[c,d]	ϕ[e,f]	relative orientation[e,g]	ref
[Fe(TMP)(1-MeIm)$_2$]ClO$_4$	1.988(20)	1.975(3)		23	0[h]	17
	1.987(1)	1.965(3)		41	0[h]	
[Fe(TPP)(HIm)$_2$]Cl·CHCl$_3$	1.994(12)	1.977(3)		6	0[h]	24
	1.993(4)	1.964(3)		41	0[h]	
[Fe(TPP)(4-MeHIm)$_2$]Cl	2.000(11)	1.975(2)		3.1	0[h]	33
	1.995(10)	1.987(2)		4.6	0[h]	33
[Fe(TPP)(t-Mu)$_2$]SbF$_6$	1.992(5)	1.983(4)		22	0[h]	34
[Fe(TPP)(c-Mu)$_2$]SbF$_6$	1.997(1)	1.967(7)		29	0[h]	34
	1.995(17)	1.979(7)		15	0[h]	
[Fe(TPP)(1-MeIm)$_2$]ClO$_4$	1.982(11)	1.974(6)[b]		22/32	11	35
[Fe(OEP)(4-NMe$_2$Py)$_2$]ClO$_4$	2.002(4)	1.995(3)		36	0[h]	17
[Fe(Proto IX)(1-MeIm)$_2$]	1.991(16)	1.977(16)[b]		3/16	13	36
paral-[Fe(TMP)(5-MeHIm)$_2$]ClO$_4$	1.983(4)	1.970(12)[b]		10/46	30	18
	1.981(5)	1.982(3)[b]		14/12	26	
paral-[Fe(OMTPP)(1-MeIm)$_2$]Cl	1.990(2)	1.996(29)[b]	0.01	12.6/6.9	19.5	37
average of the above 10	1.991(6)	1.978(10)				
[Fe(TPP)(HIm)$_2$]Cl·MeOH	1.989(8)	1.974(24)[b]	0.31	18/39	57	25
perp-[Fe(TMP)(5-MeHIm)$_2$]ClO$_4$	1.981(7)	1.965(11)[b]	0.32	30/12	76	18
[Fe(TPP)(2-MeHIm)$_2$]ClO$_4$	1.971(4)	2.012(4)[b]	0.40	32/32	89.3	15
[Fe(TMP)(1,2-Me$_2$Im)$_2$]ClO$_4$	1.937(12)	2.004(0)[b]	0.72	44.8/45.4	89.4	19
[Fe(TPP)(Py)$_2$]ClO$_4$	1.982(7)	2.003(3)[b]	0.25	34/38	86	20
[Fe(TMP)(3-ClPy)$_2$]ClO$_4$	1.968(3)	2.012(8)[b]	0.36	48/29	77	21
[Fe(TMP)(4-CNPy)$_2$]ClO$_4$	1.961(7)	2.011(14)[b]	0.41	43/44	90	22
[Fe(TMP)(3-EtPy)$_2$]ClO$_4$	1.964(4)	1.996(9)[b]	0.43	43/43	90	21
[Fe(TMP)(4-NMe$_2$Py)$_2$]ClO$_4$	1.964(10)	1.984(8)[b]	0.51	37/42	79	17
[Fe(TPP)(4-CNPy)$_2$]ClO$_4$	1.952(7)	2.002(8)[b]	0.55	35/36	89	22
average of the above 10	1.967(14)	1.996(16)				
perp-[Fe(OMTPP)(1- MeIm)$_2$]Cl	1.969(7)	1.982(10)	0.10	29.3	90.0[h]	37
[Fe(OETPP)(1-MeIm)$_2$]Cl	1.970(7)	1.977(1)[b]	0.03	9.6/82.7	73	37
[Fe(OETPP)(4-NMe$_2$Py)$_2$]Cl	1.951(5)	2.000(22)[b]	0.28	9.0/29.0	70	40
[Fe(OMTPP)(4-NMe$_2$Py)$_2$]ClO$_4$	1.979(3)	2.009[b]	0.01	1.3/2.4	84.2	38
[Fe(OMTPP)(Py)$_2$]ClO$_4$	1.973(3)	2.024(4)	0.18	23.4	90.0[h]	38
[Fe(OETPP)(4-NMe$_2$Py)$_2$]ClO$_4$	1.977(2)	2.030(3)[b]	0.08	10.6/20.5	53.2	38
average of the above 6	1.970(10)	2.004(22)				
average of the above 16	1.968(13)	1.999(18)				
perp-[Fe(OEP)(2- MeHIm)$_2$]Cl	1.974(4)	2.005(10)	0.46	40.8/43.4	87.6	this work
paral-[Fe(OEP)(2- MeHIm)$_2$]ClO$_4$	2.041(9)	2.275(1)	0.05	22.2	0[h]	26

[a] Estimated standard deviations are given in parentheses. [b] Averaged value. [c] In Å. [d] Average absolute values of displacements of the methine carbons from the 24-atom mean plane. [e] Value in degrees. [f] Dihedral angle between the plane defined by the closest N$_p$−Fe− N$_{im}$ and the imidazole plane. [g] Dihedral angle between two axial ligands. [h] Exact value required by symmetry.

dihedral angle between the two axial ligand planes. This results in a relative ligand orientation of 87.6° between the two imidazole planes. Both ligands are almost perpendicular to the porphyrin plane with dihedral angles 86.1° and 88.6°. The Fe−N$_{im}$−C$_{im}$ angles are also listed in Table 2.

The crystalline species was studied with variable temperature Mössbauer spectroscopy. The quadrupole splitting and isomer shift values show a weak temperature dependence. The quadrupole splitting for the crystalline species *perp*-[Fe(OEP)(2-MeHIm)$_2$]Cl at 295 K is 1.81 mm/s. The isomer shifts at the corresponding temperature is 0.26 mm/s. These Mössbauer parameters at various other temperatures are given in Table S7 of the Supporting Information.

Discussion

The data given below clearly show that *perp*-[Fe(OEP)-(2-MeHIm)$_2$]Cl is a low-spin species in the solid state. This is in distinct contrast with that observed for *paral*-[Fe(OEP)-(2-MeHIm)$_2$]ClO$_4$,[26] which has been shown to display a high-spin state in the crystalline state. However, as shown previously by Geiger et al.,[26] solutions of the salt [Fe(OEP)-(2-MeHIm)$_2$]ClO$_4$ display a thermal spin-equilibrium between a high-spin species and a low-spin species. It is thus clear that the complex [Fe(OEP)(2-MeHIm)$_2$]$^+$ is close to the spin crossover point and that subtle phenomena might shift the balance between the two spin states.

Structure of *perp*-[Fe(OEP)(2-MeHIm)$_2$]Cl. As shown in Figure 1, the cation is a six-coordinate species with relative perpendicular imidazole ligands. It has a ruffled core conformation, which is also shown in Figure 2, a formal diagram giving atomic displacements of core atoms from the 24-atom mean plane. The large absolute value of displacements of *meso*-carbon atoms (C$_m$) is a feature of ruffled conformations. Saddled structures usually have large displacement of β-carbon atoms but not large C$_m$ displacements. For comparison, related structural data for low-spin bis-ligated iron(III) porphyrinates are listed in Table 3. There are three groups of complexes in this table. The top group gives values for species having the two axial ligands with relative parallel orientations, while the second and third groups give values for species having the two axial ligands with relative perpendicular orientations. The top group has porphyrin core conformations that are effectively planar; the second group are largely those with strongly ruffled porphyrin cores, while the third group are extremely saddled. An estimate of the ruffling magnitude can be given by the

average displacement of C_m from the 24-atom mean plane. For the title complex, the average absolute value of C_m (0.46 Å) is in the middle of those values of ruffled iron(III) porphyrinates shown in Table 3. In this complex, a strongly ruffled porphyrin core is required in order to allow the close approach with the sterically bulky 2-methylimidazole ligands, with the formation of two oblong cavities at right angles on opposite sides of the porphyrin ring and a relative perpendicular orientation of the two axial imidazole ligands.

The average equatorial distance observed in *perp*-[Fe(OEP)(2-MeHIm)$_2$]Cl is 1.973(4) Å which is similar to those values for the ruffled and saddled structures in Table 3.[26] The average value for the equatorial Fe−N_p distances in those six-coordinate iron(III) porphyrinates with two perpendicular ligands is ∼1.968(13) Å, about ∼0.02 Å shorter than those iron(III) porphyrinates with two parallel ligands (1.991(6) Å). These former complexes have ruffled or saddled porphyrin core conformations rather than planar conformations. This decrease (bond shortening) is the clear result of the core distortion. The average value of the two axial Fe−N_{im} distances in the title complex is 2.005(10) Å, which is similar to the corresponding distances observed in other ruffled bis(imidazole-ligated) iron(III) porphyrinates (1.996(17) Å), but longer than those in planar structures (1.978(10) Å) where the two ligand planes have a relative parallel orientation.

The above structural data suggest similarity between this OEP complex and those tetraaryl porphyrin complexes shown in Table 3. When hindered methylimidazoles are used as ligands, in the low-spin structures of OEP, TPP, and TMP, they all have very ruffled porphyrin cores with two perpendicular ligands. There could be some weak interaction between imidazole atoms and methyl atoms of the mesityl groups in the TMP complex but no such interaction in TPP and OEP complexes. So the dominant factor of the ruffling must be the interaction between imidazole atoms and porphyrin core atoms. To clearly represent the interaction between imidazole atoms and the porphyrin core, the distances between imidazole hydrogen atoms and their close five-membered atom plane in the porphyrin core have been chosen as shown in Figure 3. In *perp*-[Fe(OEP)(2-MeHIm)$_2$]$^+$, H(3) and H(7) are hydrogen atoms bonded to the 4-position imidazole carbon; H(4) and H(8) are hydrogen atoms bonded to the 2-methyl carbon. These distances are listed in Table 4. The average distance is 2.34 Å between 4-position hydrogen atoms and the close plane and 2.52 Å between 2-methyl hydrogen atoms and the close plane. The corresponding distances are 2.30 and 2.48 Å for [Fe(TPP)(2-MeHIm)$_2$]ClO_4,[15] 2.34 and 2.60 Å for [Fe(TMP)(1,2-Me_2-Im)$_2$]ClO_4.[19] If the porphyrin core were planar, the calculated values were 2.22 and 2.34 Å. They are thus about 0.1 Å shorter than those found in the ruffled structures, which would cause much larger repulsion interaction between the imidazole group and the porphyrin core. The *paral*-[Fe(OEP)(2-MeHIm)$_2$]ClO_4 complex has a planar core but the H···core distances are increased by both an appropriate absolute orientation of the imidazole and an increased axial Fe−N_{im} distance of 2.275 Å appropriate for the high-spin state. Thus the steric interaction between the 2-methylimidazole and the core in high-spin *paral*-[Fe(OEP)(2-MeHIm)$_2$]ClO_4 is similar to that of *perp*-[Fe(OEP)(2-MeHIm)$_2$]Cl.

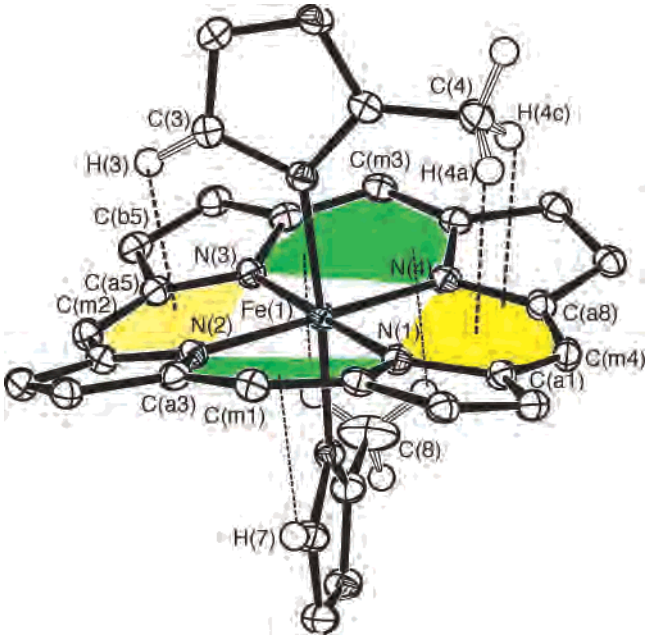

Figure 3. Diagram showing the interaction between imidazole hydrogen atoms and their close five-membered atom plane in the 24-atom core. Yellow planes are mean planes 1 and 3 that have close interactions with the hydrogen atoms of 2-methyl and 4-carbon atoms of the upper imidazole in the figure. Green planes are mean planes 2 and 4 that have close interactions with the hydrogen atoms of the lower imidazole in the figure. Dashed lines indicate the distance between hydrogen atom and the closest mean plane.

The steric interaction of the 2-methyl group adjacent to the porphyrin core atoms leads to a small tilting of the Fe−N_{im} bond from the normal to the porphyrin plane; values are 3.7 and 3.2°. The direction of the tilts always serve to minimize the imidazole methyl group···porphyrin core contacts. In addition, the methyl group leads to significantly different pairs of Fe−N_{im}−C_{im} angles; the angle involving the methyl side of imidazole is 132.85(11) and 132.54(11)°, while the unhindered C_{im} has Fe−N_{im}−C_{im} angles of 120.88(11) and 121.31(11)°. These are similar to the values in [Fe(TPP)(2-MeHIm)$_2$]$^+$,[15] where small tilt angles(∼4°) and large difference between two different Fe−N_{im}−C_{im} angles are also observed.

In comparing *perp*-[Fe(OEP)(2-MeHIm)$_2$]Cl with *paral*-[Fe(OEP)(2-MeHIm)$_2$]ClO_4,[26] one obvious difference is the counterion. For the title complex, the chloride counterion plays an important role in hydrogen bonding in the solid state as shown in Figure 4. The chloride ion (Cl(1)) is hydrogen bonded to two uncoordinated imidazole nitrogen atoms (N(6) and N(8)) from two different units and forms a one-dimensional zigzag chain. The corresponding distances, 3.16 Å (Cl(1)···N(6)) and 3.22 Å (Cl(1)···N(8)), are a little shorter than the standard hydrogen bond N···Cl distance (3.3 Å).[41] The moderately strong hydrogen bonding can make

(33) Silver, J.; Marsh, P. J.; Symons, M. C. R.; Svistunenko, D. A.; Frampton, C. S.; Fern, G. R. *Inorg. Chem.* **2000**, *39*, 2874.
(34) Quinn, R.; Valentine, J. S.; Byrn, M. P.; Strouse, C. E. *J. Am. Chem. Soc.* **1987**, *109*, 3301.
(35) Higgins, T.; Safo, M. K.; Scheidt, W. R. *Inorg. Chim. Acta* **1990**, *178*, 261.

Table 4. Selected Distances of Imidazole Hydrogen Atoms to the Corresponding Plane for *perp*-[Fe(OEP)(2-MeHIm)$_2$]Cl and Related Species

	perp-[Fe(OEP)-(2-MeHIm)$_2$]Cl	[Fe(TPP)-(2-MeHIm)$_2$]$^+$ [15]	[Fe(TMP)-(1,2-Me$_2$Im)$_2$]$^+$ [19]	*paral*-[Fe(OEP)-(2-MeHIm)$_2$]ClO$_4$ [26]
H(3)···plane 1[a](Å)	2.31	2.31	2.37	2.42[b]
H(7)···plane 2[c](Å)	2.37	2.29	2.31	
average of the above 2	2.34	2.30	2.34	
H(4a)···plane 3[d](Å)	2.46	2.36	2.57	2.63[b]
H(4c)···plane 3[d](Å)	2.56	2.55	2.63	2.65[b]
H(8a)···plane 4[e](Å)	2.47	2.41	2.57	
H(8c)···plane 4[e](Å)	2.58	2.61	2.64	
average of the above 4	2.52	2.48	2.60	

[a] Mean plane 1 is defined by N(3), C(a5), C(m2), C(a4), and N(2). [b] Two equal distances as required by inversion symmetry. [c] Mean plane 2 is defined by N(1), C(a3), C(m1), C(a2), and N(2). [d] Mean plane 3 is defined by N(1), N(4), C(m4), C(a1), and C(a8). [e] Mean plane 4 is defined by N(3), N(4), C(a6), C(m3), and C(a7).

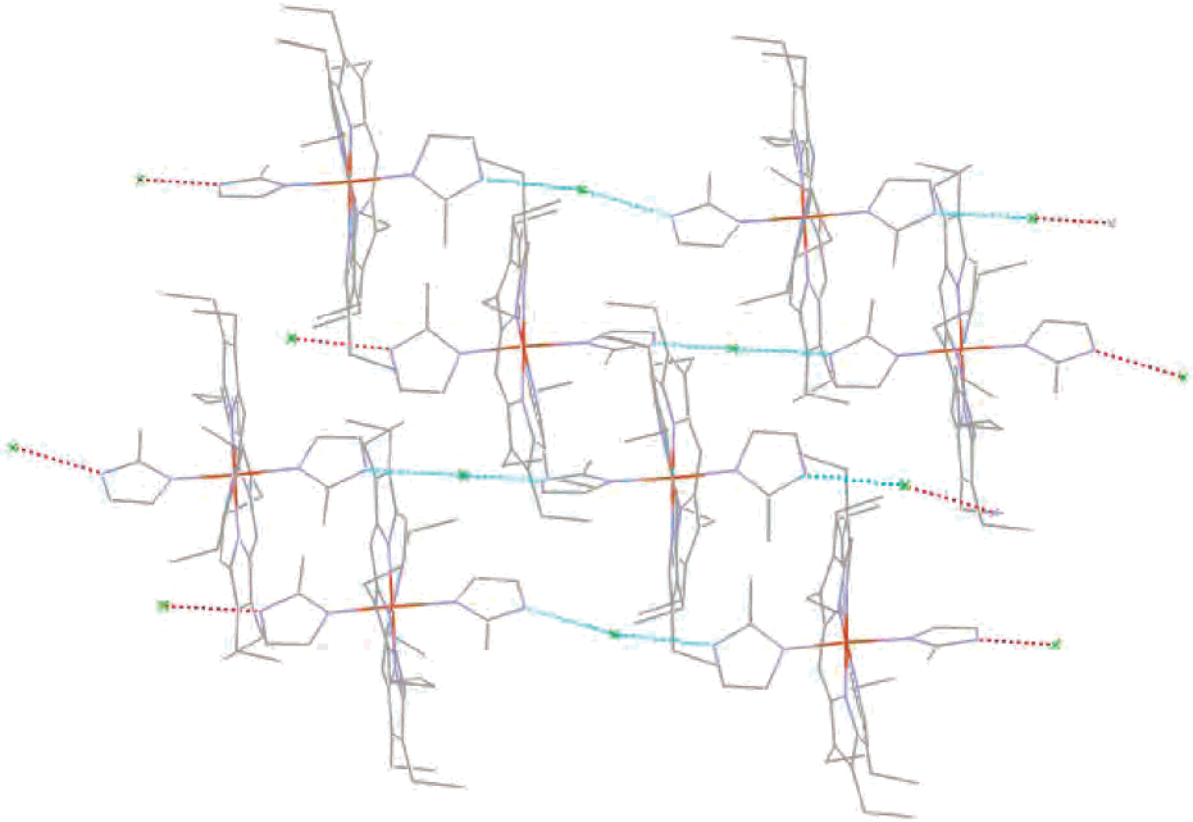

Figure 4. Hydrogen bonding network in the crystal structure of *perp*-[Fe(OEP)(2-MeHIm)$_2$]Cl.

the coordinated imidazole have some imidazolate character and thus act as a stronger ligand field.[42] For the [Fe(OEP)-(2-MeHIm)$_2$]$^+$ system, which is known to be close to the spin crossover point,[26] the hydrogen-bonding effect on the ligand field strength is apparently sufficient to favor the low-spin state observed for *perp*-[Fe(OEP)(2-MeHIm)$_2$]Cl. Interestingly, a hydrogen bond network was found for *paral*-[Fe(OEP)(2-MeHIm)$_2$]ClO$_4$[26] as shown in Figure S1. The hydrogen bonding appears weaker in this system; the perchlorate is disordered so that the H-bonding to the imidazole N−H distance is either 2.92 or 3.08 Å for N···O with the distance to the second imidazole is then 3.08 or 2.92 Å, respectively. Although other factors may well also contribute, the weaker H-bonding then leads to the high-spin state observed for *paral*-[Fe(OEP)(2-MeHIm)$_2$]ClO$_4$.[26] The hydrogen bond distances and angles for both low-spin *perp*-[Fe(OEP)(2-MeHIm)$_2$]Cl and high-spin *paral*-[Fe(OEP)-(2-MeHIm)$_2$]ClO$_4$ are listed in Table S8. Hydrogen bonding to the uncoordinated N−H group of a ligated imidazole is also known to substantially enhance the equilibrium binding constant of the ligated imidazole in iron(II) and cobalt(III) porphyrinates.[43−45]

(36) Little, R. G.; Dymock, K. R.; Ibers, J. A. *J. Am. Chem. Soc.* **1975**, *97*, 4532.
(37) Yatsunyk, L. A.; Carducci, M. D.; Walker, F. A. *J. Am. Chem. Soc.* **2003**, *125*, 15986.
(38) Ohgo, Y.; Ikeue, T.; Takahashi, M.; Takeda, M.; Nakamura, M. *Eur. J. Inorg. Chem.* **2004**, *798*.
(39) Epstein, L. M.; Straub, D. K.; Maricondi, C. *Inorg. Chem.* **1967**, *6*, 1720.
(40) Ogura, H.; Yatsunyk, L.; Medforth, C. J.; Smith, K. M.; Barkigia, K. M.; Renner, M. W.; Melamed, D.; Walker, F. A. *J. Am. Chem. Soc.* **2001**, *123*, 6564.
(41) Hamilton, W. C.; Ibers, J. A. In *Hydrogen Bonding in Solids: Methods of Molecular Structure Determination*; Hamilton, W. C., Ed.; W. A. Benjamin: New York, 1968.
(42) Reed, C. A.; Mashiko, T.; Bentley, S. P.; Kastner, M. E.; Scheidt, W. R.; Spartalian, K.; Lang, G. *J. Am. Chem. Soc.* **1979**, *101*, 2948.

Table 5. Solid-State Mössbauer Parameters for the Title Complex and Related Species

complex	ΔE_q[a]	δ_{Fe}[a]	sample phase	T (K)	relative orientation[b]	conf[c]	ref
			Type I				
perp-[Fe(OEP)(2-MeHIm)$_2$]Cl	1.85	0.20	cryst solid		87.6	ruf	this work
[Fe(TMP)(4-NMe$_2$Py)$_2$]ClO$_4$	1.74	0.20	cryst solid	77	79	ruf	17
perp-[Fe(TMP)(5-MeHIm)$_2$]ClO$_4$	1.78	0.22	cryst solid	120	76	ruf	18
[Fe(TPP)(2-MeHIm)$_2$]ClO$_4$	1.77	0.22	cryst solid	120	89.3	ruf	16
[Fe(TMP)(1,2-Me$_2$Im)$_2$]ClO$_4$	1.26	0.17	cryst solid	120	89.4	ruf	19
[Fe(TMP)(2-MeHIm)$_2$]ClO$_4$	1.48	0.20	cryst solid	77	*e*	*e*	21
[Fe(TMP)(3-EtPy)$_2$]ClO$_4$	1.25	0.18	cryst solid	77	90	ruf	21
[Fe(TMP)(3-ClPy)$_2$]ClO$_4$	1.36	0.20	cryst solid	77	77	ruf	21
[Fe(TPP)(Py)$_2$]Cl	1.25	0.16	solid	77	*e*	*e*	39
perp-[Fe(OMTPP)(1-MeIm)$_2$]Cl	1.70	0.27	cryst solid	4.2	90	sad	46
[Fe(OETPP)(1-MeIm)$_2$]Cl	1.94	0.26	cryst solid	4.2	73	sad	46
[Fe(OETPP)(4-NMe$_2$Py)$_2$]Cl	2.13	0.26	cryst solid	4.2	70	sad	46
[Fe(OMTPP)(4-NMe$_2$Py)$_2$]ClO$_4$	1.89	0.23	cryst solid	70	84	sad	38
[Fe(OMTPP)(Py)$_2$]ClO$_4$	2.18	0.25	cryst solid	78	90	sad	38
[Fe(OETPP)(4-NMe$_2$Py)$_2$]ClO$_4$	2.31	0.26	cryst solid	80	53	sad	38
			Type II				
paral-[Fe(TMP)(5-MeHIm)$_2$]ClO$_4$	2.56	0.22	cryst solid	120	26/30	pla	18
[Fe(TMP)(1-MeHIm)$_2$]ClO$_4$	2.28	0.28	cryst solid	77	0	pla	17
[Fe(OEP)(4-NMe$_2$Py)$_2$]ClO$_4$	2.14	0.26	cryst solid	77	0	pla	17
[Fe(TPP)(4-MeHIm)$_2$]Cl	2.26	0.34	cryst solid	77	0	pla	33
[Fe(TPP)(HIm)$_2$]Cl	2.23	0.23	crystalline(?)	77	*d*	*d*	39
paral-[Fe(OMTPP)(1-MeIm)$_2$]Cl	2.78	0.28	cryst solid	4.2	19.5	sad	46
			Type III				
[Fe(TMP)(4-CNPy)$_2$]ClO$_4$	0.97	0.20	cryst solid	77	70	ruf	21
[Fe(TPP)(4-CNPy)$_2$]ClO$_4$	0.65	0.19	cryst solid	4.2	89	ruf	22

[a] mm/s. [b] Dihedral angle between two axial ligands. [c] Predominant core conformation contribution: pla, planar; ruf, ruffled; sad, saddled. [d] Not determined, presumed parallel and planar. [e] Not determined, presumed perpendicular and ruffled.

Mössbauer Spectra. Among the bis-ligated Fe(III) porphyrinates with imidazole or pyridine as ligands, three structural/spectroscopic categories can be identified: (Type I) perpendicular ligands, normally ruffled or saddled porphyrin core, with "large g_{max}" EPR, and quadrupole splittings usually in the range from 1.2 to 1.8 mm/s; (Type II) parallel ligands, usually planar porphyrin cores although a saddled example exists, with classic rhombic EPR and quadrupole splittings in the range from 2.1 to 2.8 mm/s; and (Type III) axial ligands nearly perpendicular, ruffled porphyrin core, axial EPR spectrum, very small quadrupole splitting. Type I and Type II have the ground state $(d_{xy})^2(d_{xz},d_{yz})^3$; type III has the ground state $(d_{xz},d_{yz})^4(d_{xy})^1$.

For the title complex, Mössbauer spectra were measured from room temperature to 20 K. The isomer shift (0.26 mm/s) indicates it is a low-spin species. Both quadrupole splitting and isomer shift are typical for type I compounds, which suggests that the electronic ground state is $(d_{xy})^2(d_{xz},d_{yz})^3$. Table 5 shows the strong similarity between the Mössbauer data observed for the current complex and related species. The Mössbauer spectra clearly show that *perp*-[Fe(OEP)(2-MeHIm)$_2$]Cl undergoes significant magnetic broadening. Line widths at RT are somewhat broadened to 0.40 and 0.54 mm/s but are broadened to 1.05 and 1.02 mm/s at 20 K. This broadening is likely due to unresolved magnetic hyperfine interactions with intermediate fluctuation rates on the Mössbauer time scale. The failure to see an EPR spectrum, even at 4.2 K, could be related to this magnetic broadening, either through a spin-state equilibrium or through incipient intermolecular magnetic coupling. We note that some compounds in Type I have ΔE_q larger than 1.8 mm/s. These porphyrins all have strongly saddled cores, which could be the reason for the larger ΔE_q values. A comparison of ΔE_q of the planar species with the same porphyrin (for example, 2.8 mm/s for *paral*-[Fe(OMTPP)(1-MeIm)$_2$]Cl), shows that the saddled species with relative perpendicular axial ligands still have much smaller quadrupole splitting values.

Summary. The synthesis and isolation of a six-coordinate bis(2-methylimidazole)(octaethylporphyrinato)iron(III) chloride, *perp*-[Fe(OEP)(2-MeHIm)$_2$]Cl, has been accomplished. This complex has been characterized by an X-ray diffraction study. Distinct from the high-spin *paral*-[Fe(OEP)(2-MeHIm)$_2$]ClO$_4$ derivative,[26] this complex is a low-spin iron(III) porphyrinate with its axial ligands in a relative perpendicular orientation. Consistent with the necessary use of a hindered imidazole to achieve a relative perpendicular orientation, the porphyrin core is strongly ruffled. This complex has been found to have shorter equatorial Fe−N$_p$ bonds and longer Fe−N$_{im}$ bonds than those found in analogous planar complexes that have the two axial imidazoles in a relative parallel orientation. A one-dimension hydrogen-bond chain is formed between chloride anions and uncoordinated imidazole nitrogen atoms. Mössbauer spectroscopy verified the low-spin state of the species and confirmed that it is a type I low-spin species with ground state $(d_{xy})^2(d_{xz},d_{yz})^3$.

(43) Coyle, C. L.; Rafson, P. A.; Abbott, E. H. *Inorg. Chem.* **1973**, *12*, 2007.
(44) Walker, F. A.; Lo, M.-W.; Ree, M. T. *J. Am. Chem. Soc.* **1976**, *98*, 5552.
(45) Balch, A. L.; Watkins, J. J.; Doonan, D. J. *Inorg. Chem.* **1979**, *18*, 1228.
(46) Teschner, T.; Yatsunyk, L.; Schü×b6nemann, V.; Paulsen, H.; Winkler, H.; Hu, C.; Scheidt, W. R.; Walker, F. A.; Trautwein, A. X. *J. Am. Chem. Soc.* **2006**, *128*, 1379.

Acknowledgment. We thank the National Institutes of Health for support of this research under Grant GM-38401 and the NSF for X-ray instrumentation (CHE-0443233).

Supporting Information Available: Tables S1−S6, giving complete crystallographic details, atomic coordinates, bond distances and angles, anisotropic temperature factors, and fixed hydrogen atom positions; Table S7 showing variable-temperature Mössbauer parameters; Table S8 showing hydrogen bond distances and angles for *perp*-[Fe(OEP)(2-MeHIm)$_2$]Cl and *paral*-[Fe(OEP)(2-MeHIm)$_2$]ClO_4; Figure S1 showing the hydrogen bonding network in the structure of *paral*-[Fe(OEP)(2-MeHIm)$_2$]ClO_4; X-ray crystallographic file. This material is available free of charge via the Internet at http://pubs.acs.org.

IC061014U